



Published in final edited form as:

Oncogene. 2011 May 19; 30(20): 2345–2355. doi:10.1038/onc.2010.605.

IL-6 promotes prostate tumorigenesis and progression through autocrine cross-activation of IGF-IR

Andres Rojas¹, Gang Liu¹, Ilsa Coleman², Peter S. Nelson², Miqin Zhang³, Rupesh Dash⁴, Paul B Fisher⁴, Stephen R. Plymate¹, and Jennifer D. Wu¹

¹ Department of Medicine, University of Washington, Seattle, WA

² Fred Hutchinson Cancer Research Center, Seattle, WA

³ Department of Material Science and Engineering, University of Washington, Seattle, WA

⁴ Department of Human and Molecular Genetics, VCU Institute of Molecular Medicine and VCU Massy Cancer Center, Virginia Commonwealth University, Richmond, VA

Abstract

As an established mediator of inflammation, IL-6 is implicated to facilitate prostate cancer progression to androgen independence through transactivation of the androgen receptor. However, whether IL-6 plays a causative role in *de novo* prostate tumorigenesis was never investigated. We now provide the first evidence that IL-6 can induce tumorigenic conversion and further progression to an invasive phenotype of non-tumorigenic benign prostate epithelial cells. Moreover, we find that paracrine IL-6 stimulates autocrine IL-6 loop and autocrine activation of IGF-IR to confer the tumorigenic property and that activation of STAT3 is critical in these processes. Inhibition of STAT3 activation or IGF-IR signaling suppresses IL-6-mediated malignant conversion and the associated invasive phenotype. Inhibition of STAT3 activation suppresses IL-6-induced upregulation of IGF-IR and its ligands IGF-I and IGF-II. These findings indicate IL-6 signaling cooperates with IGF-IR signaling in the prostate microenvironment to promote prostate tumorigenesis and progression to aggressiveness. Our findings suggest that STAT3 and IGF-IR may represent potential effective targets for prevention or treatment of prostate cancer.

Keywords

IL-6; STAT3; tumorigenesis; EMT; IGF-IR; prostate

Users may view, print, copy, download and text and data- mine the content in such documents, for the purposes of academic research, subject always to the full Conditions of use: http://www.nature.com/authors/editorial_policies/license.html#terms

Corresponding Author: Jennifer D. Wu, Ph. D, Box 359625, 325 9th Ave, Seattle, WA 98104, Phone: (206) 897 5349, Fax: (206) 897 5302, wuj@uw.edu.

Conflict of Interest

The authors declare no conflict of interest.

Introduction

Emerging evidence suggests that chronic or recurrent prostate inflammation may initiate and promote prostate cancer development (Bardia *et al.*, 2009; De Marzo *et al.*, 2007; Haverkamp *et al.*, 2008; Sutcliffe and Platz, 2007). However, rational chemoprevention or treatment of prostate cancer with anti-inflammatory drugs has not been fully exploited, in part due to the lack of understanding of the molecular and cellular mechanisms by which inflammation influences prostate carcinogenesis (Bardia *et al.*, 2009).

The pleiotropic cytokine IL-6 is produced by various inflammatory cells in tissue microenvironment through activation of the inflammatory transcriptional nuclear factor NF κ B (Grivennikov and Karin, 2008). As an established major mediator of inflammation, IL-6 has been suggested to facilitate prostate cancer progression to androgen-independent disease and potentially to promote bone metastasis (Ara and Declerck, 2010; Corcoran and Costello, 2003; Ishiguro *et al.*, 2009; Paule *et al.*, 2007; Santer *et al.* 2010). Elevated level of serum IL-6 or persistent activation of the IL-6 signaling components STAT3 in prostate carcinomas has been correlated with the shortened survival of prostate cancer patients (Nakashima *et al.*, 2000; Tam *et al.*, 2007). These studies suggested the significance of IL-6 in prostate cancer malignant progression to advanced diseases. However, whether IL-6 plays a causative role in facilitating the progression from pre-malignant states to overt malignancy remains unclear.

In the present study we demonstrate that IL-6 can induce tumorigenic conversion of immortal but non-tumorigenic prostate epithelium, a process accompanied by an epithelial to mesenchymal transition (EMT) leading to an invasive phenotype, through activation of STAT3. Interestingly, we find that IL-6 exposure not only stimulates IL-6 autocrine loop but also lead to activation of insulin-like type I growth factor receptor (IGF-IR) signaling through autocrine secretion of IGF-IR ligands IGF-I and IGF-II and upregulation of IGF-IR expression. Moreover, we find that activation of STAT3 is critical in establishing the autocrine network of IL-6 and IGF axis. To our knowledge, this is the first report linking the pro-inflammatory cytokine IL-6 with endocrine IGF axis in facilitating prostate malignancy and the overt progression to an invasive phenotype.

Results

IL-6 induces EMT of benign prostate epithelial cells

To understand the role of IL-6 in prostate tumorigenesis, we treated the SV40T-immortalized benign non-tumorigenic prostate epithelial cell line P69 with IL-6 at the concentration of 10, 20, 50 or 100 ng/ml. After 24 h exposure, P69 cells exhibited a spindle-like depolarized fibroblast-like morphology at all concentrations of IL-6 (Figure 1A and data not shown). This morphology and related properties persisted for at least five passages in culture after withdraw of IL-6 (Supplemental Figure S1). Immunofluorescence staining and Western blot analyses demonstrated that the morphological changes were associated with gain of the molecular features of EMT (Zeisberg and Neilson, 2009), such as loss of E-cadherin and induction of Vimentin (Figures 1A and 1B). Concomitantly, real-time RT-PCR analyses showed that changes in gene expression patterns were consistent with EMT,

including repression of E-Cadherin and induction of Vimentin, N-cadherin, and Snail in P69 cells treated with IL-6 compared to control untreated cells (Figure 1C).

We further determined that IL-6 induced similar changes in the expression of E-Cadherin and/or Vimentin in the immortalized non-tumorigenic BPH-1 cells and primary prostate epithelial cells (Supplemental Figure S2). These observations suggest that the effects of IL-6 on P69 cells represent a general effect of IL-6 on prostate epithelial cells, not a cell line-specific effect.

Increased cell migration is one of the characteristics of cells undergoing EMT. Accordingly, we evaluated the migratory potential of P69 cells in the presence or absence of IL-6 in wounding assays. Cell monolayers were incised and then exposed to serum-free medium supplemented with IL-6 or serum. Wound closure was measured at early time points, such as 12 hours, which were representative of migration rather than proliferation. In the presence of IL-6, P69 cells demonstrated markedly increased migration compared to serum controls (Figure 1D).

IL-6 induces EMT through activation of STAT3 and IGF-IR signaling

IL-6 signals through a specific IL-6 receptor and a promiscuous transmembrane signal transducer, gp130, to activate the JAK2/STAT3 pathway (Corcoran and Costello, 2003). As shown in Figure 2A, exposure to IL-6 induced phosphorylation of STAT3 and associated loss of E-cadherin in P69 cells. In the presence of the STAT3 inhibitor AG490, IL-6 showed no or a minimal effect on E-Cadherin expression. These data suggested a key role of STAT3 activation in IL-6 induction of EMT.

Inflammatory cytokines have been shown to act through cell surface growth factor receptor pathways (Al-Shanti *et al.*, 2008; Colomiere *et al.*, 2009; Corcoran and Costello, 2003; Soon *et al.*, 1999). IL-6 has been shown to induce EMT in ovarian carcinomas through cross-activation of STAT3 and the epidermal growth factor receptor (EGFR) which is frequently overexpressed in ovarian cancers (Colomiere *et al.*, 2009). As IGF-IR plays an important role in the tumorigenesis and neoplastic growth of prostate (Kojima *et al.*, 2009; Werner and Bruchim, 2009), we are thus motivated to investigate if IGF-IR plays a role in the induction of EMT by IL-6. As shown by Western blotting analyses (Figure 2B) and immunofluorescence staining (Figure 2C), blocking IGF-IR with a specific antibody IMC-A12 abrogated or markedly reduced the effect of IL-6 on E-Cadherin and Vimentin expression in P69 and BPH-1 cells, whereas treatment these cells with IMC-A12 alone had no or a minimal effect on E-Cadherin or Vimentin expression. These results suggested that IGF-IR signaling plays a critical role in IL-6 induction of EMT.

IL-6 induction of EMT is associated with gain of malignant phenotypes

EMT has recently proposed to be a central process for cancer development, progression, and metastasis (Thiery, 2002; Thiery *et al.*, 2009). Thus, undergoing EMT may signify the acquisition of a malignant phenotype which in prostate epithelial cells can be distinguished from a non-malignant phenotype by the morphological structures formed in three-dimensional (3-D) Matrigel cultures (Zhang *et al.*, 2009). We examined the morphological

suggest that IL-6 has the potential to facilitate tumorigenesis of benign non-tumorigenic prostate epithelial cells and that STAT3 and IGF-IR play critical roles in such an event.

IL-6 facilitates *in vivo* tumorigenesis and metastatic progression

A more stringent assay for malignant phenotype is the ability to form a tumor *in vivo*. We thus overexpressed IL-6 in P69 and BPH-1 cells (designated as P69^{IL-6} and BPH-1^{IL-6}) and implanted these cells subcutaneously into immune-deficient athymic nude mice. Consistent with previous reports, parental P69 and BPH-1 cells (with the empty vector) did not form tumors in nude mice in a three-month post-implantation analysis period (Figures 5A and 5B). In contrast, tumors were formed within 10 days of inoculation in all animals implanted with P69^{IL-6} or BPH-1^{IL-6} cells (Figure 5A).

We further addressed the metastatic potential of tumors formed by P69^{IL-6} or BPH-1^{IL-6} cells by removing primary tumors from animals through survival surgery at six weeks post-inoculation. Metastasis was observed in the lymph nodes of all the tumor-bearing animals in a two-week post-surgery follow-up, as confirmed by SV40T-antigen (SV40Tag) immunostaining of these tissues (Figure 5C). Vimentin was abundantly expressed in both the primary and the metastasized tumors (Figure 5C), consisting with the *in vitro* observed feature associated with EMT. These data confirm that IL-6 can not only induce tumorigenic conversion but also promote tumor progression to metastasis.

Activation of STAT3 is critical for autocrine loop of IL-6 and activation of IGF-IR

To investigate the mechanisms by which IL-6 may act through IGF-IR signaling, we first examined the activation status of IGF-IR in P69 cells with IL-6 treatment. Without exogenous ligands IGF-I or IGF-II, IGF-IR was phosphorylated only at a basal level in serum-free media to maintain the viability of the cells (Figure 6A; (Damon *et al.*, 2001). In the presence of IL-6, phosphorylation of IGF-IR was markedly increased without addition of exogenous IGF-I or IGF-II; moreover, the phosphorylation was inhibited by the STAT3 inhibitor AG490 (Figure 6A). Semi-quantitative real-time RT-PCR demonstrated that IL-6 upregulated the expression of IGF-I and IGF-II (Figures 6B and 6C) as well as IGF-IR (Figure 6D). Similarly, this effect of IL-6 was inhibited by the STAT3 inhibitor AG490. Moreover, IL-6 also stimulated P69 cells to produce autocrine IL-6 and to upregulate the expression of IL-6 signaling components, gp130 and IL-6R through STAT3 activation (Figures 6E–6G). Similar effects of IL-6 were also observed in BPH-1 cells (Supplement Figure S3). These results demonstrate that paracrine IL-6 can stimulate autocrine activation of IGF-IR and engage an autocrine IL-6 loop and that activation of STAT3 is critical in maintaining these autocrine activities.

Transcriptional reprogramming of benign prostate epithelial cells by IL-6

To identify potential genetic changes underlying IL-6-mediated tumorigenesis and associated EMT, we examined the transcriptional re-programming of P69 cells exposed to IL-6 using 44K whole human genome expression oligo microarray analyses. We identified an array of genes were upregulated and a cohort of 176 genes that were significantly upregulated ($q^2 < 0.05$) in P69 cells following IL-6 treatment (Figure 7A and data not shown). These include panels of known genes encoding inflammation related cytokines and

chemokines, extracellular matrix components, transcription factors, and tumorigenesis-associated factors (Supplement Table S1). The significant upregulation of IL-6 and EMT-associated hallmarks, e.g. N-Cadherin, Vimentin, and Snail, as exhibited by the microarray analyses is consistent with the data as described above throughout our experiments. We also validated the upregulated expression of the two well-studied carcinogenesis-associated genes, K-Ras and Lipocalin 2 (LCN2), by quantitative RT-PCR (Figure 7B). Mutations or overexpression of the oncogene K-RAS have been associated with tumorigenesis (Karnoub and Weinberg, 2008; Rosen *et al.*, 2006; Traynor *et al.*, 2008). LCN2 has been shown to induce EMT of breast cancer cells and promote tumor growth and progression (Berger *et al.*, ; Yang *et al.*, 2009). Furthermore, blocking IGF-IR signaling with the antibody IMC-A12 or blocking STAT3 activation with AG490 significantly inhibited IL-6-induced upregulation of K-Ras and LCN2 (Figures 7B). These data suggest that IL-6 induces a reprogramming of cellular transcriptional activity and upregulates the expression of a spectrum of genes that are critical for tumor initiation and progression. The data also suggest that STAT3 and IGF-IR activation plays a significant role in IL-6-induced reprogramming of cellular transcription.

Discussion

IL-6 has been shown to trans-activate androgen receptor in prostate cancer cells through STAT3 pathway to facilitate androgen-independence (Corcoran and Costello, 2003; Ishiguro *et al.*, 2009). Here, for the first time we demonstrate that IL-6 plays a causal role in *de novo* prostate tumorigenesis and malignant progression to invasiveness of otherwise non-tumorigenic benign prostate epithelial cells. More interestingly, we demonstrate that IL-6 facilitates tumorigenesis and progression through a novel pathway, the autocrine activation of IGF-IR. We demonstrate that IL-6 and the IGF axis form a potent autocrine network through activation of STAT3. This is the first report demonstration the network of inflammatory cytokine IL-6 and the autocrine IGF axis in promoting prostate tumorigenesis.

Here we demonstrate that IL-6 induces an EMT in association with the gain of malignancy of benign prostate epithelial cells. IL-6 has also been shown to facilitate breast tumor growth and metastasis through induction of EMT (Sullivan *et al.*, 2009). Although the pathways of EMT in epithelial cancers are not fully understood, activation of an EMT program has been proposed as the critical mechanism for the acquisition of invasiveness and metastasis (Kang and Massague, 2004). Consistent with this concept, autocrine expression of IL-6 in benign P69 and BPH-1 cells resulted in not only transformation and *in vivo* tumor formation, but also tumor progression to metastasis. Our findings are consistent with those in colitis-associated cancers, which showed that IL-6 was not only important for early tumor development, but also critical for late stage tumor progression (Becker *et al.*, 2004; Grivennikov *et al.*, 2009).

IL-6 is also a result of obesity which is associated with an increased risk of developing aggressive prostate cancer and mortality (Freedland and Platz, 2007). Periprostatic adipose tissue has been shown to be a major source of IL-6 and indicated to facilitate the development of high grade prostate cancer through IL-6 signaling (Finley *et al.*, 2009). Although the underlying biological mechanism is not fully understood, it has been

speculated that the association of obesity with increasing prostate cancer aggressiveness may be resulted from endocrine derangements (Irigaray *et al.*, 2007; O'Malley and Taneja, 2006). Our data revealed that paracrine IL-6 in the prostate microenvironment, resulted from inflammation or periprostatic adipose tissues, can instigate a vicious endocrine loop of IL-6 and thus maintain a sustained endocrine activation of the IGF-IR through persistent activation of STAT3. Our data has defined one of the mechanisms by which obesity may be associated with prostate endocrine derangement and prostate cancer progression to aggressiveness.

IL-6 has been proposed as a target for treating androgen-independent prostate cancer. Here we demonstrate a critical role of IL-6 in prostate cancer development and a potential role in facilitating progression to metastasis. Thus, targeting IL-6 signaling pathway may also be of particular interest in prostate cancer prevention and treatment or prevention of metastatic diseases. However, clinical trial with an anti-IL-6 monoclonal antibody CNTO328 in prostate cancer patients with advanced diseases did not present adequate efficacy (Dorff *et al.*). The poor therapeutic outcome with the anti-IL-6 antibody may be in part due to the overriding vicious autocrine loop of IL-6, and possibly IGF axis in malignant tumor cells as we have shown. Given the critical role of STAT3 in maintaining the autocrine IL-6 loop and activating IGF-IR during prostate cancer tumorigenesis and malignant progression as we have presented here, targeting STAT3, potentially in combination with targeting IGF-IR, may be an alternative strategy to an anti-IL-6 antibody in perturbing IL-6 signaling for advanced prostate cancer treatment or inflammation-associated prostate cancer prevention.

Materials and Methods

Cell lines and culture

The generation and characterization of the benign non-tumorigenic prostate epithelial cell line P69 has been described (Bae *et al.*, 1994). The benign human prostate epithelial cell line BPH-1 was obtained from the American Type Cell Culture (Manassas, VA). Cells were maintained in RPMI 1460 media supplemented with 10% fetal bovine serum, 100 units/ml penicillin, and 100 µg/ml streptomycin. For IL-6 treatment, cells were cultured in serum free media with IL-6 of indicated concentration with or without the presence of IGF-IR blocking antibody IMC-A12 (Burtrum *et al.*, 2003; Rowinsky *et al.*, 2007) for the period as indicated. The IMC-A12 antibody is IGF-IR specific and does not react with insulin receptor (Rowinsky *et al.*, 2007). The Stat3 inhibitor AG490 (Cayman Chemical) was resuspended in DMSO and a final concentration of 10 µM was used.

Proliferation assay

Cells were seeded in a 96-well plate at the density of 2,500 cells/well in serum-free media for 24 h before addition of 50 ng/ml of IL-6 and/or IMC-A12 antibody. Proliferation was quantified after 48 h by a colorimetric MTS tetrazolium (MTT) assay using the Cell Titer 96 AQueous kit (Promega) as described (Coe *et al.*, 2007). Eight replicates were performed for each experiment.

Three-dimensional (3-D) Matrigel culture

Three-dimensional cultures were prepared as described (Zhang *et al.*, 2009). Briefly, cells (1×10^6) were mixed with 1 mL undiluted Matrigel and seeded in a six-well culture dish. After polymerization at 37 °C for 1 h, the Matrigel/cell mixture was overlaid with appropriate medium. The same batch of Matrigel was used throughout this study. Medium was replaced every three days. Cultures were grown for up to 15 days.

Immunofluorescence

For two-dimensional (2-D) culture, cells were plated onto sterile round microscope slides in 24-well plates and grown to 70% confluence. After washing, cells were fixed with 4% paraformaldehyde for 30 min at 4°C. After three washes, cells were blocked with 5% non-fat milk for 1h at RT followed by incubating with an anti-E-cadherin mouse monoclonal antibody (mAb) (kindly provided by Dr William Carter at the Fred Hutchinson Cancer Research Center) or/and an anti-Vimentin rabbit monoclonal antibody SP20 (Lab Vision) o/n at 4°C. After several washes, cells were incubated with an Alexa fluor® 488-conjugated (Invitrogen) or Alexa fluor® 594-conjugated (Invitrogen) secondary antibodies for 1h. DAPI (5µg / ml) was used to stain nuclei. Slides were mounted with SlowFade (Invitrogen).

For staining of the 3-D culture, a sample (~10 µl) of Matrigel culture was spread on each well of a 4-well chamber slide, air dried, and fixed in 1:1 methanol/acetone at 20°C for 10 min. After washing with PBS, the slides were incubated with the blocking solution, primary antibodies, and fluorochrome-conjugated secondary reagents as described above. Slides were visualized under a LZM5100 confocal microscope. Representative pictures were shown from experiments repeated at least twice with 20 to 50 morphologic structures analyzed.

Western Blots

Cells were lysed in cold lysis buffer (30 mM HEPES, 150 mM NaCl, 1.5 mM MgCl₂, 1 mM EGTA, 10% Triton X-100) containing Protease and Phosphatase Inhibitor Cocktail II (Sigma, St. Louis, MO). 25 µg of clear cell lysates of each sample was resolved in a 10–14% SDS-PAGE gel and transferred to a nitrocellulose membrane. After blocking with 5% nonfat milk in TBST buffer (20 mM Tris-HCl, pH 7.5, containing 0.15 M NaCl, 0.5% 0.1% Tween 20), blots were incubated overnight at 4°C with appropriate antibodies followed with horseradish peroxidase-linked secondary antibodies (Cell Signaling). Proteins were detected using enhanced chemiluminescence reagents (ECL, Amersham). Antibodies specifically to the following molecules were used: pSTAT3 (Cell Signaling), total STAT3 (Cell Signaling), E-cadherin (a gift from Dr. William Carter, Fred Hutchinson Cancer Research Center, Seattle, WA), Vimentin (Lab Vision Products), phospho-IGF-IR (Boisource), IGF-IR (Santa Cruz), and GAPDH (Cell Signaling).

Quantitative RT-PCR (qRT-PCR)

Total RNA was extracted using TRizol (Invitrogen). cDNA was synthesized using the SuperScript II kit (Invitrogen). 1 µl of cDNA were mixed with Power SYBR® Green PCR MasterMix (Applied Biosystems) and specific primers sets were added to a final

concentration of 400 nM in 20 μ l of reaction mixture. The reaction was run on an ABI9700 machine and data was analyzed Lightcycler software v3.5. Each sample was assayed in triplicates. Target mRNA levels were normalized against GAPDH. The primers used are listed in Supplemental Table S2.

Wound assay

Cells were plated in six-well plates with complete RPMI 1460 medium and grown to confluence. After rinsing the cells twice with PBS, the cell layer was scratched with a 10- μ l pipette tip and overlaid with serum-free RPMI 1460 in the presence or absence of 50 ng/ml of IL-6. Wound width was measured at 0, 12, and 24 hours after wounding.

Anchorage Independent Growth

Anchorage-independent cell growth was assayed by the capacity of cells to form colonies in soft agar as described in detail elsewhere (Bae *et al.*, 1994). Briefly, 1×10^4 cells were plated on Petri dishes in 0.3% agar/media. The number and size of colonies were documented at indicated time points.

Plasmids, transfection, and PEG-3 promoter luciferase reporter assay

The construction of PEG-3 promoter-Luciferase plasmid (pPEG3-Luc) and luciferase assay were previously described (Su *et al.*, 2000; Su *et al.*, 2001; Su *et al.*, 2005). Cells were transiently transfected with pPEG3-Luc plasmid using Lipofectamine 2000 (Invitrogen). Luciferase assays were performed 48 h post-transfection.

Isolation and overexpression of IL-6

cDNA of human IL-6 was amplified by PCR from P69 cells after exposure to IL-6. The following primers were used: (Forward) 5' TCT CGA GAG CCC AGC TAT GAA CTC-3' and (Reverse) 5'ATA GCG GCC GCT TAC TAC ATT TGC CGA AGA-3'. After sequence confirmation, the cDNA of IL-6 was subcloned into the retroviral vector pBMN-IRES-GFP (Orbigen Inc) which contains a cDNA for GFP as a reporter. The construct was transfected into the Ampho-Phoenix packaging cell line (Orbigen Inc). Retroviral was produced according to the manufactures' protocol and used to transduce target cells. GFP positive cells were isolated by flow cytometry sorting. Expression of IL-6 was confirmed by RT-PCR.

In vivo Tumorigenicity and Progression

All studies were done according to the regulation of IACUC protocol. 2×10^6 cells were injected subcutaneously into the right flanks of five- to six-week-old nude male mice (Harlan-Sprague-Dawley, Indianapolis, IN). Seven to eight mice were in each group. Mice were monitored twice weekly for tumor growth. Primary tumors were removed and collected by survival surgery six weeks post-inoculation. Mice were sacrificed two weeks after removal of primary tumors to examine metastasis. At sacrifice, lymph node, lung, liver, and bone were collected. All tissues were formalin-fixed, and paraffin-embedded for histological examination.

Immunohistochemistry

Paraffin embedded slides were deparaffinized. Antigen was unmasked by incubation in 95°C water bath in 10 mM sodium citrate buffer (pH 6.0) for 2 × 5 min. Slides were incubated with primary antibody specific to Vimentin (clone SP20, Lab Vision) or SV40Tag (Santa Cruz Biotechnology) in PBS containing 1% BSA and 10% goat serum. Biotinylated secondary antibodies (PharMingen) were added and incubated at room temperature for 1 hr. Streptavidin-HRP (PharMingen) was added and after 40 min the sections were stained with DAB substrate and counterstained with hematoxylin.

Microarray analysis

Total RNA was extracted as above. mRNA was amplified using the Ambion MessageAmp II Amplification Kit (Ambion Inc.), labeled, and hybridized to Agilent 44K whole human genome expression oligonucleotide microarray slides following manufacturer's protocols (Agilent Technologies, Inc.). Fluorescent array images were collected using the Agilent DNA microarray scanner G2565BA. Data was analyzed using Agilent Feature Extraction software. Statistical Analysis of Microarray (SAM) program (Tusher *et al.*, 2001), with a false discovery rate (FDR) of <5% considered significant.

Statistical Analysis

Student's t-test was performed to determine statistically significant differences between groups, and a P-value of 0.05 was considered significant.

Supplementary Material

Refer to Web version on PubMed Central for supplementary material.

Acknowledgments

This work was supported by National Institute of Health (NIH) Temin Award 1K01CA116002, NIH 1R01CA149405, and DOD-USARMC IDEA Development Award W81XWH-06-1-0014 to J.W. and partially supported by the Pacific Northwest Prostate Cancer SPORE P50-CA097186 (J.W.) and NIH Program Project Grant PO1 CA085859 (S.R.P) and P01 CA104177 (P.B.F). P.B.F. holds the Thelma Newmeyer Corman Chair in Cancer Research at the VCU Massey Cancer Center.

References

- Al-Shanti N, Saini A, Faulkner SH, Stewart CE. Beneficial synergistic interactions of TNF-alpha and IL-6 in C2 skeletal myoblasts--potential cross-talk with IGF system. *Growth Factors*. 2008; 26:61–73. [PubMed: 18428025]
- Ara T, Declerck YA. Interleukin-6 in bone metastasis and cancer progression. *Eur J Cancer*.
- Bae VL, Jackson-Cook CK, Brothman AR, Maygarden SJ, Ware JL. Tumorigenicity of SV40 T antigen immortalized human prostate epithelial cells: association with decreased epidermal growth factor receptor (EGFR) expression. *Int J Cancer*. 1994; 58:721–9. [PubMed: 8077059]
- Bardia A, Platz EA, Yegnasubramanian S, De Marzo AM, Nelson WG. Anti-inflammatory drugs, antioxidants, and prostate cancer prevention. *Curr Opin Pharmacol*. 2009; 9:419–26. [PubMed: 19574101]
- Becker C, Fantini MC, Schramm C, Lehr HA, Wirtz S, Nikolaev A, et al. TGF-beta suppresses tumor progression in colon cancer by inhibition of IL-6 trans-signaling. *Immunity*. 2004; 21:491–501. [PubMed: 15485627]

- Berger T, Cheung CC, Elia AJ, Mak TW. Disruption of the *Lcn2* gene in mice suppresses primary mammary tumor formation but does not decrease lung metastasis. *Proc Natl Acad Sci U S A*. 2003; 100:2995–3000. [PubMed: 12536303]
- Burtrum D, Zhu Z, Lu D, Anderson DM, Prewett M, Pereira DS, et al. A fully human monoclonal antibody to the insulin-like growth factor I receptor blocks ligand-dependent signaling and inhibits human tumor growth in vivo. *Cancer Res*. 2003; 63:8912–21. [PubMed: 14695208]
- Coe KJ, Jia Y, Ho HK, Rademacher P, Bammler TK, Beyer RP, et al. Comparison of the cytotoxicity of the nitroaromatic drug flutamide to its cyano analogue in the hepatocyte cell line TAMH: evidence for complex I inhibition and mitochondrial dysfunction using toxicogenomic screening. *Chem Res Toxicol*. 2007; 20:1277–90. [PubMed: 17702527]
- Colomiere M, Ward AC, Riley C, Trenerry MK, Cameron-Smith D, Findlay J, et al. Cross talk of signals between EGFR and IL-6R through JAK2/STAT3 mediate epithelial-mesenchymal transition in ovarian carcinomas. *Br J Cancer*. 2009; 100:134–44. [PubMed: 19088723]
- Corcoran NM, Costello AJ. Interleukin-6: minor player or starring role in the development of hormone-refractory prostate cancer? *BJU Int*. 2003; 91:545–53. [PubMed: 12656913]
- Damon SE, Plymate SR, Carroll JM, Sprenger CC, Dechsukhum C, Ware JL, et al. Transcriptional regulation of insulin-like growth factor-I receptor gene expression in prostate cancer cells. *Endocrinology*. 2001; 142:21–7. [PubMed: 11145562]
- De Marzo AM, Platz EA, Sutcliffe S, Xu J, Gronberg H, Drake CG, et al. Inflammation in prostate carcinogenesis. *Nat Rev Cancer*. 2007; 7:256–69. [PubMed: 17384581]
- Dorff TB, Goldman B, Pinski JK, Mack PC, Lara PN Jr, Van Veldhuizen PJ Jr, et al. Clinical and correlative results of SWOG S0354: a phase II trial of CNT0328 (siltuximab), a monoclonal antibody against interleukin-6, in chemotherapy-pretreated patients with castration-resistant prostate cancer. *Clin Cancer Res*. 2008; 14:3028–34. [PubMed: 1844019]
- Finley DS, Calvert VS, Inokuchi J, Lau A, Narula N, Petricoin EF, et al. Periprostatic adipose tissue as a modulator of prostate cancer aggressiveness. *J Urol*. 2009; 182:1621–7. [PubMed: 19683746]
- Freedland SJ, Platz EA. Obesity and prostate cancer: making sense out of apparently conflicting data. *Epidemiol Rev*. 2007; 29:88–97. [PubMed: 17478439]
- Grivennikov S, Karin E, Terzic J, Mucida D, Yu GY, Vallabhapurapu S, et al. IL-6 and Stat3 are required for survival of intestinal epithelial cells and development of colitis-associated cancer. *Cancer Cell*. 2009; 15:103–13. [PubMed: 19185845]
- Grivennikov S, Karin M. Autocrine IL-6 signaling: a key event in tumorigenesis? *Cancer Cell*. 2008; 13:7–9. [PubMed: 18167335]
- Haverkamp J, Charbonneau B, Ratliff TL. Prostate inflammation and its potential impact on prostate cancer: a current review. *J Cell Biochem*. 2008; 103:1344–53. [PubMed: 17955503]
- Irigaray P, Newby JA, Lacomme S, Belpomme D. Overweight/obesity and cancer genesis: more than a biological link. *Biomed Pharmacother*. 2007; 61:665–78. [PubMed: 18035514]
- Ishiguro H, Akimoto K, Nagashima Y, Kojima Y, Sasaki T, Ishiguro-Imagawa Y, et al. aPKC λ /iota promotes growth of prostate cancer cells in an autocrine manner through transcriptional activation of interleukin-6. *Proc Natl Acad Sci U S A*. 2009; 106:16369–74. [PubMed: 19805306]
- Kang Y, Massague J. Epithelial-mesenchymal transitions: twist in development and metastasis. *Cell*. 2004; 118:277–9. [PubMed: 15294153]
- Karnoub AE, Weinberg RA. Ras oncogenes: split personalities. *Nat Rev Mol Cell Biol*. 2008; 9:517–31. [PubMed: 18568040]
- Kojima S, Inahara M, Suzuki H, Ichikawa T, Furuya Y. Implications of insulin-like growth factor-I for prostate cancer therapies. *Int J Urol*. 2009; 16:161–7. [PubMed: 19183230]
- Long RM, Morrissey C, Fitzpatrick JM, Watson RW. Prostate epithelial cell differentiation and its relevance to the understanding of prostate cancer therapies. *Clin Sci (Lond)*. 2005; 108:1–11. [PubMed: 15384949]
- Nakashima J, Tachibana M, Horiguchi Y, Oya M, Ohigashi T, Asakura H, et al. Serum interleukin 6 as a prognostic factor in patients with prostate cancer. *Clin Cancer Res*. 2000; 6:2702–6. [PubMed: 10914713]
- O'Malley RL, Taneja SS. Obesity and prostate cancer. *Can J Urol*. 2006; 13(Suppl 2):11–7. [PubMed: 16672123]

- Paule B, Terry S, Kheuang L, Soyeux P, Vacherot F, de la Taille A. The NF-kappaB/IL-6 pathway in metastatic androgen-independent prostate cancer: new therapeutic approaches? *World J Urol.* 2007; 25:477–89. [PubMed: 17541600]
- Rosen DG, Yang G, Bast RC Jr, Liu J. Use of Ras-transformed human ovarian surface epithelial cells as a model for studying ovarian cancer. *Methods Enzymol.* 2006; 407:660–76. [PubMed: 16757360]
- Rowinsky EK, Youssoufian H, Tonra JR, Solomon P, Burtrum D, Ludwig DL. IMC-A12, a human IgG1 monoclonal antibody to the insulin-like growth factor I receptor. *Clin Cancer Res.* 2007; 13:5549s–5555s. [PubMed: 17875788]
- Santer FR, Malinowska K, Culig Z, Cavarretta IT. Interleukin-6 trans-signalling differentially regulates proliferation, migration, adhesion and maspin expression in human prostate cancer cells. *Endocr Relat Cancer.* 17:241–53. [PubMed: 19966016]
- Soon L, Flechner L, Gutkind JS, Wang LH, Baserga R, Pierce JH, et al. Insulin-like growth factor I synergizes with interleukin 4 for hematopoietic cell proliferation independent of insulin receptor substrate expression. *Mol Cell Biol.* 1999; 19:3816–28. [PubMed: 10207105]
- Su Z, Shi Y, Fisher PB. Cooperation between AP1 and PEA3 sites within the progression elevated gene-3 (PEG-3) promoter regulate basal and differential expression of PEG-3 during progression of the oncogenic phenotype in transformed rat embryo cells. *Oncogene.* 2000; 19:3411–21. [PubMed: 10918598]
- Su Z, Shi Y, Friedman R, Qiao L, McKinstry R, Hinman D, et al. PEA3 sites within the progression elevated gene-3 (PEG-3) promoter and mitogen-activated protein kinase contribute to differential PEG-3 expression in Ha-ras and v-raf oncogene transformed rat embryo cells. *Nucleic Acids Res.* 2001; 29:1661–71. [PubMed: 11292838]
- Su ZZ, Sarkar D, Emdad L, Duigou GJ, Young CS, Ware J, et al. Targeting gene expression selectively in cancer cells by using the progression-elevated gene-3 promoter. *Proc Natl Acad Sci U S A.* 2005; 102:1059–64. [PubMed: 15647352]
- Su ZZ, Shi Y, Fisher PB. Subtraction hybridization identifies a transformation progression-associated gene PEG-3 with sequence homology to a growth arrest and DNA damage-inducible gene. *Proc Natl Acad Sci U S A.* 1997; 94:9125–30. [PubMed: 9256446]
- Sullivan NJ, Sasser AK, Axel AE, Vesuna F, Raman V, Ramirez N, et al. Interleukin-6 induces an epithelial-mesenchymal transition phenotype in human breast cancer cells. *Oncogene.* 2009; 28:2940–7. [PubMed: 19581928]
- Sutcliffe S, Platz EA. Inflammation in the etiology of prostate cancer: an epidemiologic perspective. *Urol Oncol.* 2007; 25:242–9. [PubMed: 17483023]
- Tam L, McGlynn LM, Traynor P, Mukherjee R, Bartlett JM, Edwards J. Expression levels of the JAK/STAT pathway in the transition from hormone-sensitive to hormone-refractory prostate cancer. *Br J Cancer.* 2007; 97:378–83. [PubMed: 17595657]
- Thiery JP. Epithelial-mesenchymal transitions in tumour progression. *Nat Rev Cancer.* 2002; 2:442–54. [PubMed: 12189386]
- Thiery JP, Acloque H, Huang RY, Nieto MA. Epithelial-mesenchymal transitions in development and disease. *Cell.* 2009; 139:871–90. [PubMed: 19945376]
- Traynor P, McGlynn LM, Mukherjee R, Grimsley SJ, Bartlett JM, Edwards J. An increase in N-Ras expression is associated with development of hormone refractory prostate cancer in a subset of patients. *Dis Markers.* 2008; 24:157–65. [PubMed: 18334737]
- Tusher VG, Tibshirani R, Chu G. Significance analysis of microarrays applied to the ionizing radiation response. *Proc Natl Acad Sci U S A.* 2001; 98:5116–21. [PubMed: 11309499]
- Werner H, Bruchim I. The insulin-like growth factor-I receptor as an oncogene. *Arch Physiol Biochem.* 2009; 115:58–71. [PubMed: 19485702]
- Yang J, Bielenberg DR, Rodig SJ, Doiron R, Clifton MC, Kung AL, et al. Lipocalin 2 promotes breast cancer progression. *Proc Natl Acad Sci U S A.* 2009; 106:3913–8. [PubMed: 19237579]
- Zeisberg M, Neilson EG. Biomarkers for epithelial-mesenchymal transitions. *J Clin Invest.* 2009; 119:1429–37. [PubMed: 19487819]

Zhang X, Fournier MV, Ware JL, Bissell MJ, Yacoub A, Zehner ZE. Inhibition of vimentin or beta1 integrin reverts morphology of prostate tumor cells grown in laminin-rich extracellular matrix gels and reduces tumor growth in vivo. *Mol Cancer Ther.* 2009; 8:499–508. [PubMed: 19276168]

Author Manuscript

Author Manuscript

Author Manuscript

Author Manuscript

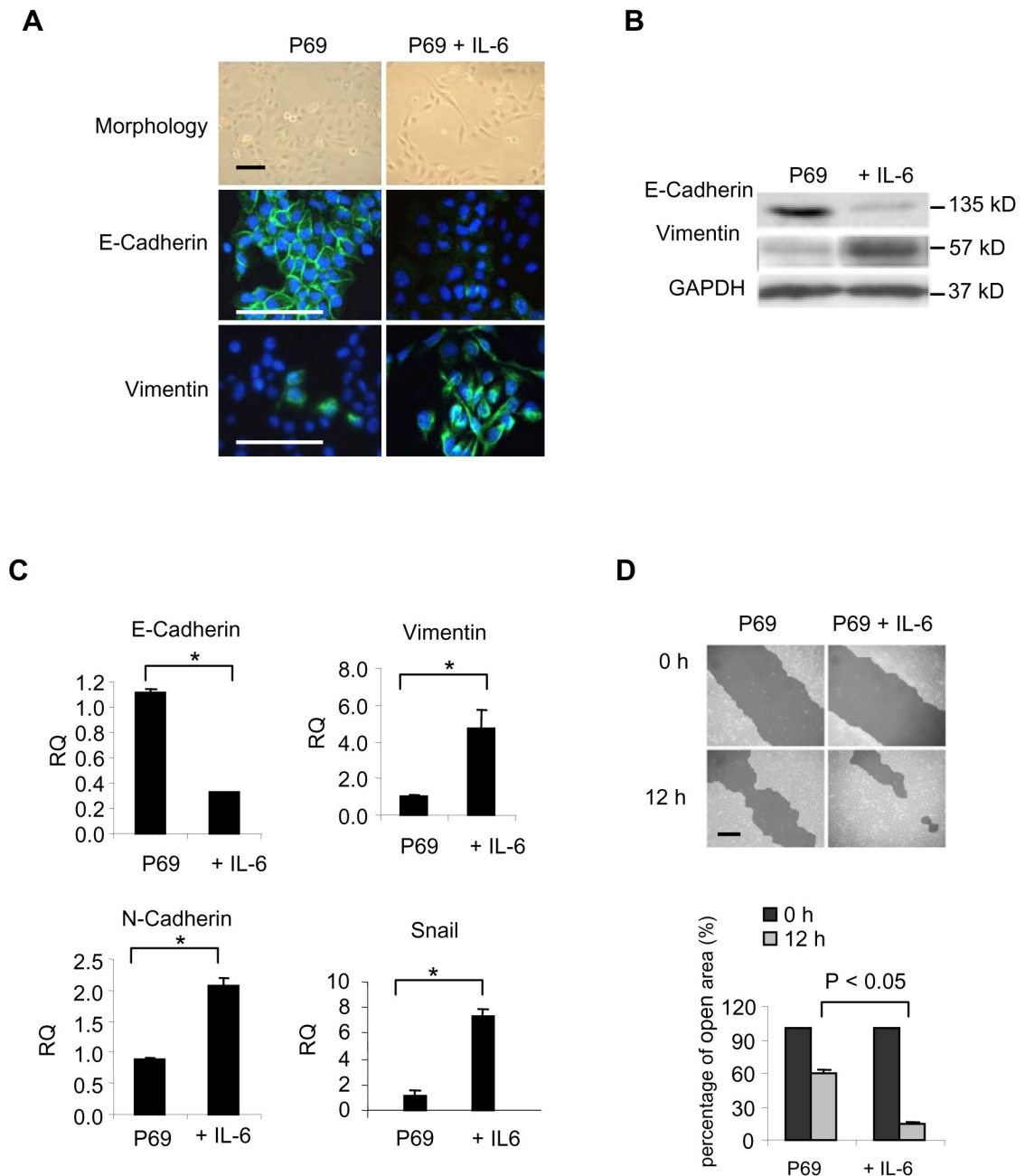


Figure 1.

IL-6 induces EMT in SV40T immortalized benign prostate epithelia P69 cells. **A**, Microscopic images demonstrating depolarized morphology and loss of E-cadherin and gain of Vimentin expression in P69 cells after exposure to IL-6. Scale bar, 100 μ m. **B**, Western blotting confirming reduction in E-cadherin and increase in Vimentin expression in P69 cells after exposure to IL-6. GAPDH was used as the loading control. **C**, Real-time RT-PCR demonstrating the changes in expression of EMT-associated genes in 69 cells after exposure to IL-6 (50 ng/ml), including E-cadherin, Vimentin, N-Cadherin, and the transcriptional factor Snail. RQ, relative quantity. **D**, Representative micrographs (top panel) and statistical

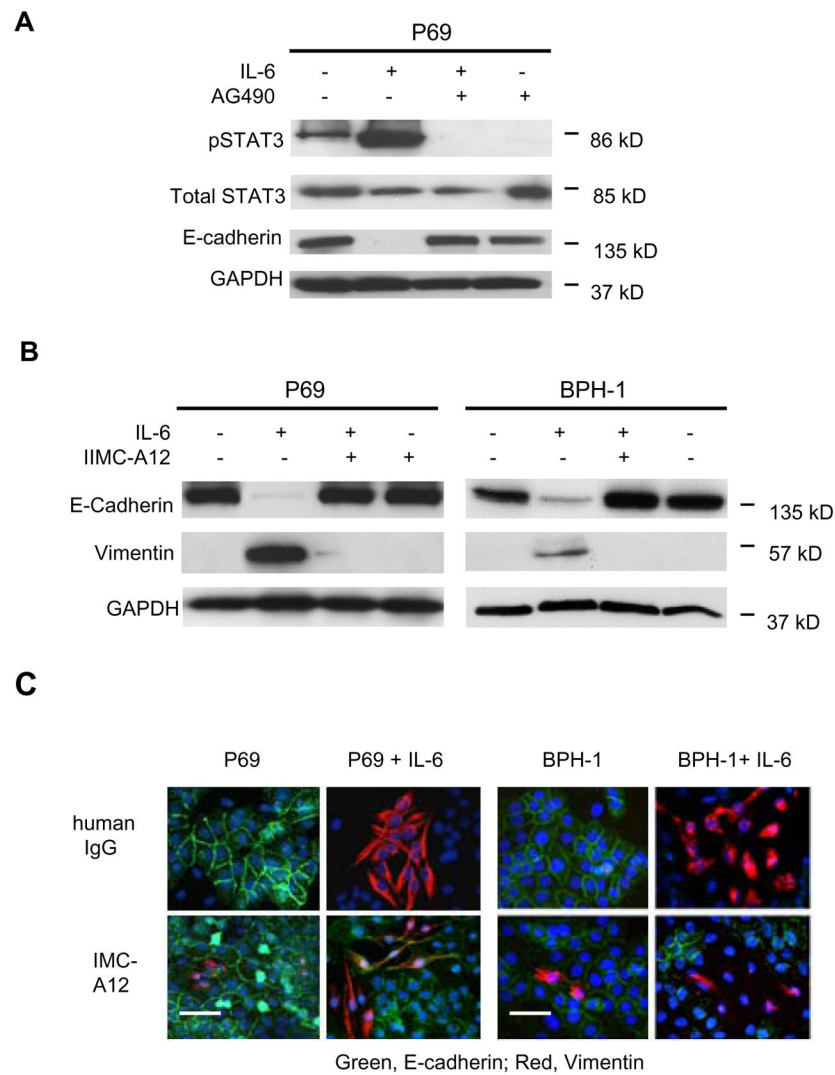
analysis (bottom panel) of wounding assay demonstrate increased migration of P69 cells in the presence of IL-6. Scale bar, 250 μm . Data expressed as mean + s.d. *, $P < 0.05$. Data shown are experiments with 50 ng/ml of IL-6.

Author Manuscript

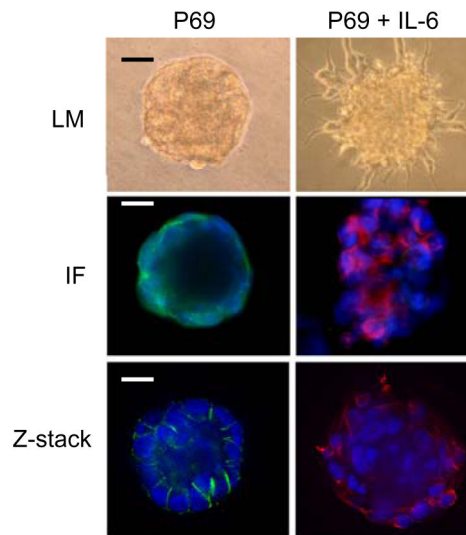
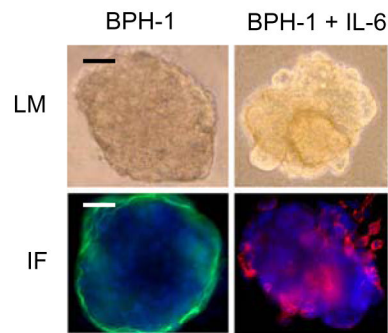
Author Manuscript

Author Manuscript

Author Manuscript

**Figure 2.**

IL-6 induces EMT through activation of STAT3 and IGF-IR. **A**, Western blotting shows that phosphorylation of STAT3 is required for IL-6-induced loss of E-Cadherin in P69 cells. Blocking STAT3 phosphorylation with AG594 inhibits the change of E-Cadherin in P69 cells. **B**, Western blotting shows that IGF-IR signaling is involved in IL-6 induced changes of Vimentin and E-Cadherin in P69 and BPH-1 cells. **C**, immunofluorescence staining demonstrates that IGF-IR signaling is critical for IL-6 induced-EMT in P69 and BPH-1 cells. Scale bar, 50 μ m. Blocking IGF-IR signaling with the monoclonal antibody (mAb) IMC-A12 inhibits loss of E-cadherin and gain of Vimentin.

A**B**

Green, E- cadherin; Red, Vimentin

Figure 3. IL-6 induces changes in three-dimensional (3-D) acini formation and malignant phenotypes of benign prostate epithelial P69 (A) and BPH-1 (B) cells in association with EMT. **Top panel,** micrographs demonstrate the morphology of acini spheres formed in 3-D Matrigel. **Middle Panel,** immunofluorescence staining demonstrates IL-6-induced changes in E-Cadherin (Green) and Vimentin (Red) in 3-D Matrigel culture. **Bottom Panel,** representative sections observed under confocal microscopy. Scale bar, 50 μ m.

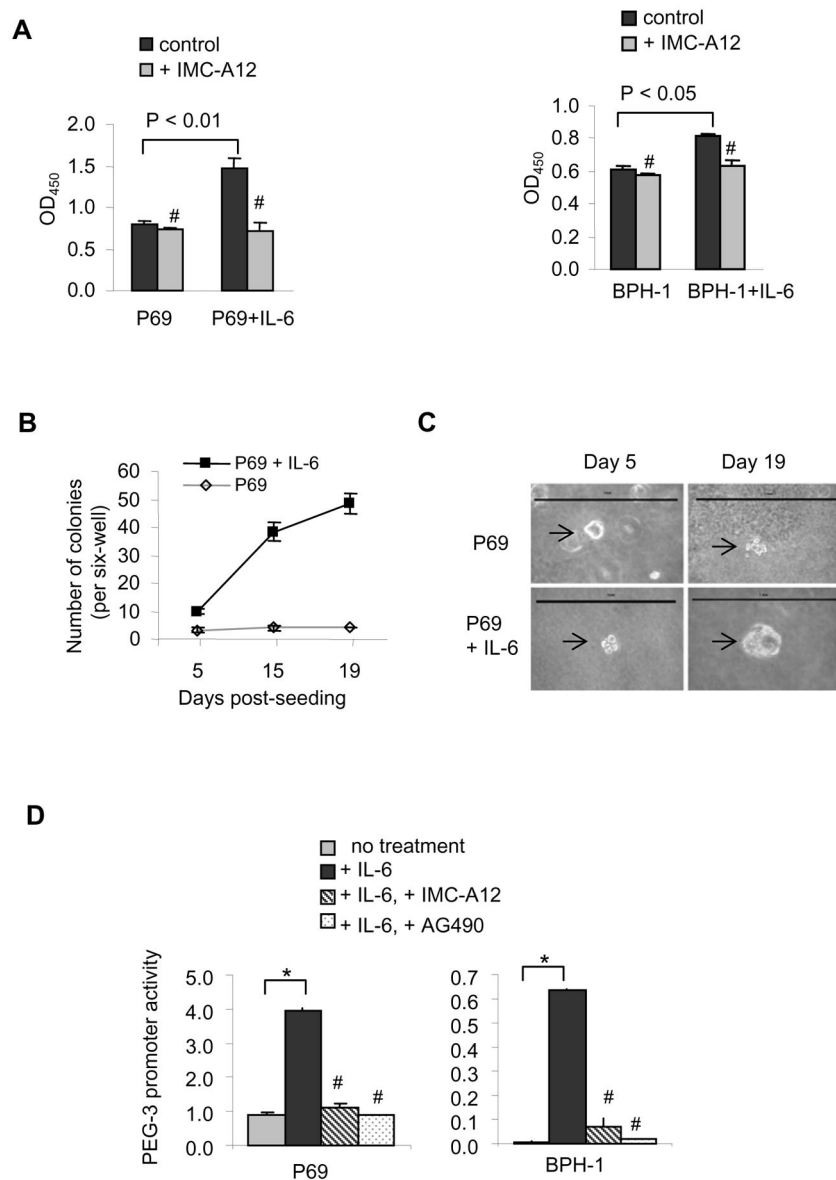


Figure 4. IL-6 induces transformation of benign P69 and BPH-1 cells through activation of IGF-IR. **A**, MTT assay (mean \pm s.d.) showing that IL-6 (50 ng/ml) stimulates proliferation of P69 and BPH-1 cells and the mitogenic effect is blocked by the anti-IGF-IR mAb IMC-A12. **B** and **C**, IL-6 facilitates colony formation of P69 cells in soft agar. **B**, numbers of colonies formed by P69 cells in the presence of IL-6 at indicated time points. **C**, representative size of colonies formed by P69 cells in the presence of IL-6 at indicated time points. Scale bar, 5mm. **D**, Reporter assay showing markedly increased transcriptional activation of the cancer-specific promoter PEG-3 in P69 and PBH-1 cells in the presence of IL-6. Data also show that inhibition of STAT3 activation with AG490 or blocking IGF-IR signaling with the mAb IMC-A12 inhibits the effect of IL-6. *, $P < 0.01$. #, not significantly different from the control.

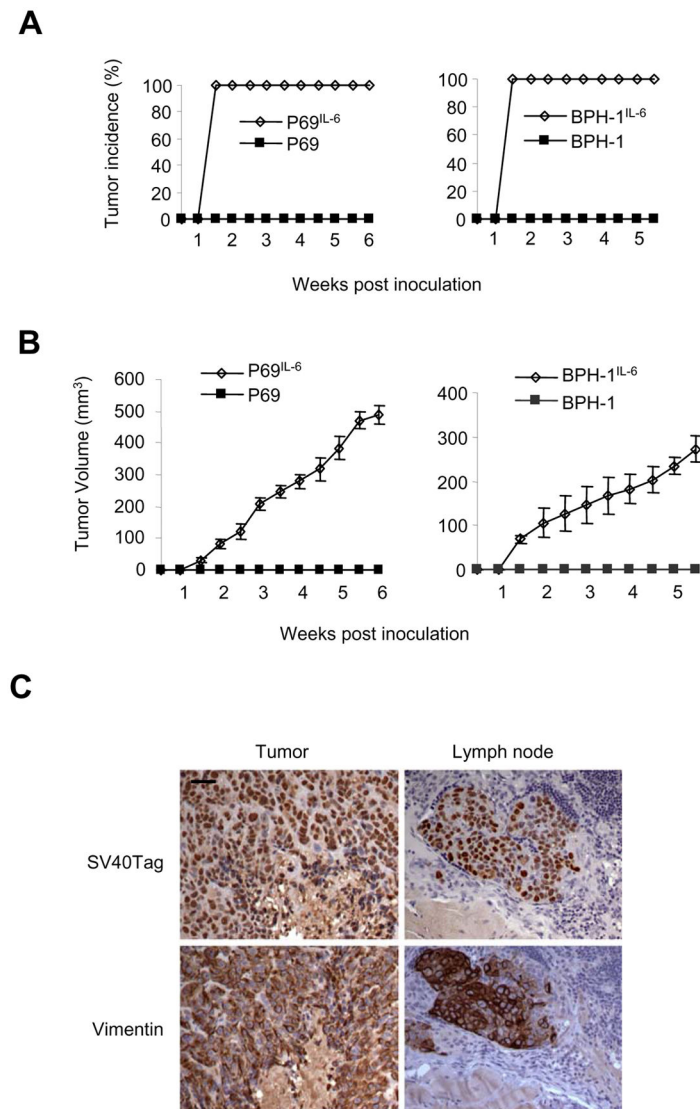
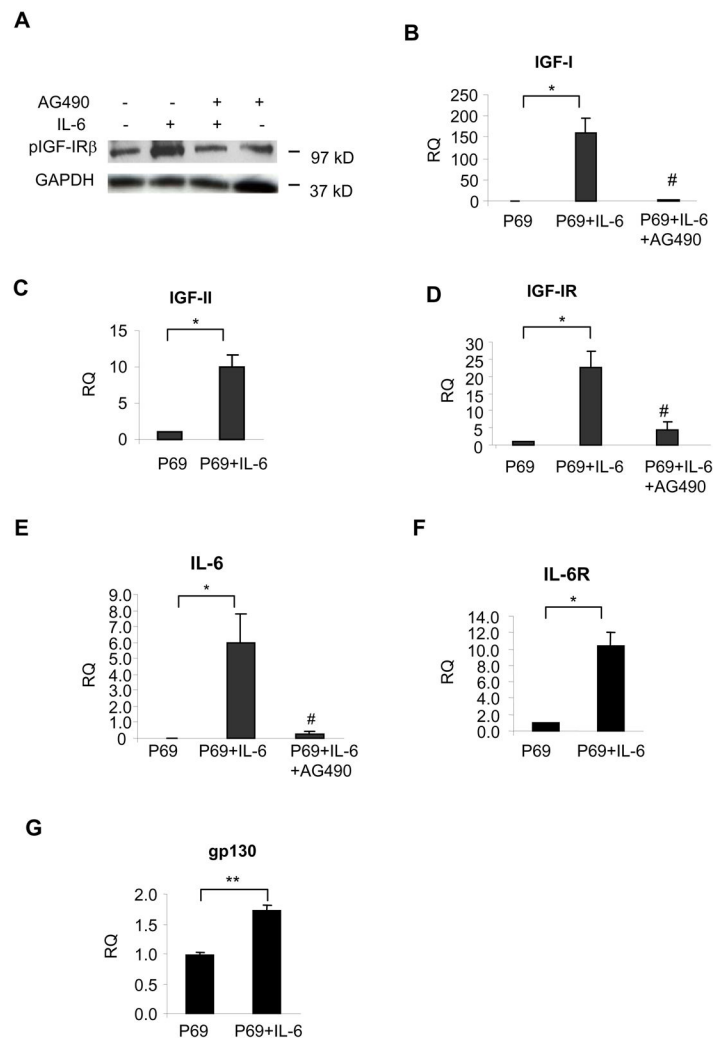


Figure 5. IL-6 promotes progressive tumorigenesis and metastatic progression of benign immortalized prostate epithelial cells *in vivo*. Human IL-6 was stably expressed in benign P69 and BPH-1 cells (designated as P69^{IL-6} and BPH-1^{IL-6} respectively). 2×10^6 /mouse P69^{IL-6} or BPH-1^{IL-6}, or parental P69 or BPH-1 cells were s.c. implanted into groups of nude mice. **A**, Tumor incidence in animals that were implanted with P69^{IL-6} or BPH-1^{IL-6} stable genetically modified cells or parental P69 or BPH-1 cells. Data show that all the animals that were implanted with P69^{IL-6} or BPH-1^{IL-6} cells developed tumors within 10 days, whereas no tumor was formed in animals that were implanted with parental P69 or BPH-1 cells. **B**, growth and volume of tumors (mean \pm s.e.) formed by P69^{IL-6} and BPH-1^{IL-6} cells. **C**, IHC staining of SV40T-Ag and Vimentin showing that tumors formed by P69^{IL-6} cells metastasized to the lymph node and that Vimentin was abundantly expressed in these tumors. Scale bar, 100 μ m.

**Figure 6.**

IL-6 induces autocrine activation of IGF-IR and autocrine loops of IL-6 signaling in P69 cells. **A**, Western blotting showing that IL-6 (50 ng/ml) induces markedly increased phosphorylation of IGF-IR in P69 cells in serum-free cultures and the effect was blocked by the STAT3 inhibitor AG490. β -tubulin was used as the loading control. **B–D**, Real-time RT-PCR showing that IL-6 induces increased expression of the ligands IGF-I and IGF-II and the receptor IGF-IR in P69 cells. Data also show that the effect of IL-6 was blocked by the STAT3 inhibitor AG490. **E–G**, Real-time RT-PCR showing that IL-6 stimulates autocrine IL-6 loop through upregulation of expression of IL-6 and its signaling components IL-6R and gp130. Data shown as mean \pm s.d. RQ, relative quantity. *, $P < 0.001$. **, $P < 0.05$. #, not significantly different from the control.

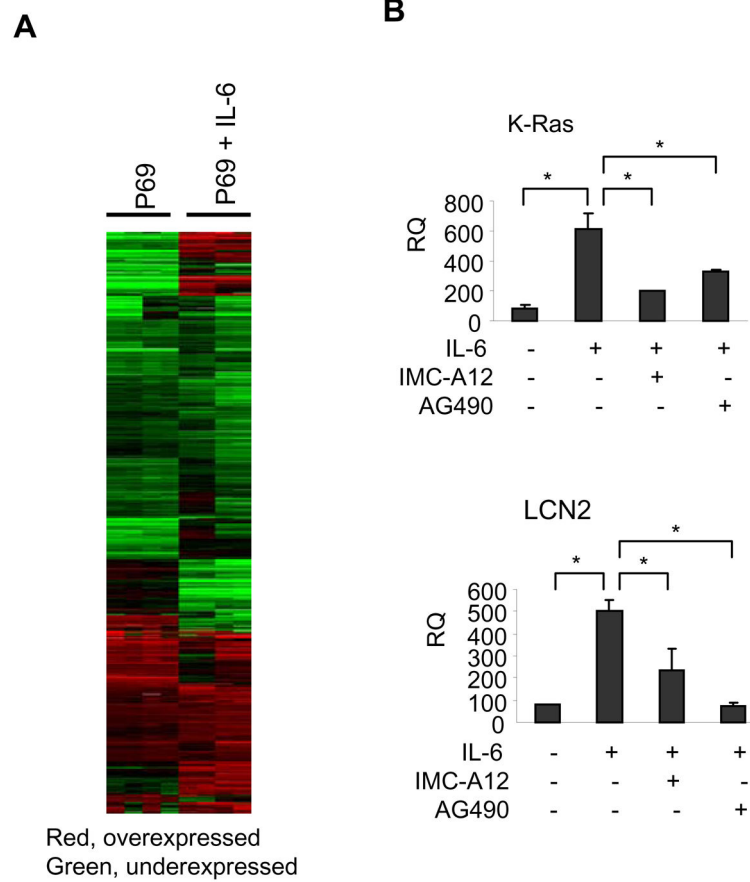


Figure 7. Transcriptional re-programming induced by IL-6 to facilitate tumorigenesis. **A**, Microarray expression profile showing clusters of genes that are upregulated by IL-6. A list of significantly upregulated genes with known function is shown in Supplemental Table 1. **B**, Real-time RT-PCR validating the upregulated expression of the two malignancy-associated genes, K-Ras and LCN2. Data also show that IL-6-induced upregulation of K-Ras and LCN2 was inhibited by blocking IGF-IR signaling with antibody IMC-A12 or STAT3 inhibitor AG490. *, $P < 0.05$.